PCCP

ROYAL SOCIETY OF CHEMISTRY

PAPER

View Article Online
View Journal | View Issue

Cite this: *Phys. Chem. Chem. Phys.*, 2023, **25**, 26327

Exploring the impact of sodium salts on hydrotropic solubilization†

Jordana Benfica, Afonso C. Martins, Germán Peréz-Sanchéz, Nicolas Schaeffer * and João A. P. Coutinho *

Received 3rd May 2023,
Accepted 8th September 2023

DOI: 10.1039/d3cp02034g

rsc.li/pccp

Some ionic liquids (ILs) were shown to display a strong ability to enhance the solubility of phenolic compounds through hydrotropy. However, evidence shows that salt ions in hydrotropic aqueous solutions may change the behavior of molecules by promoting possible interactions between the components of the system, thus causing changes in solubility. Herein, we study the impact of sodium salt anions on the hydrotropic dissolution of syringic acid using 1-butyl-3-methylimidazolium chloride ([C_4mim]Cl) as a hydrotrope, with a focus on dicyanamide Na[$N(CN)_2$] and thiocyanate Na[SCN] salts. Dynamic light scattering, Raman spectroscopy, and nuclear magnetic resonance spectroscopy were used to investigate how the mixture of IL-salts affects the solvation. The results obtained show that [C_4mim]Cl is able to increase the solubility of syringic acid 80-fold. Despite their structural similarities, the presence of Na[$N(CN)_2$] or Na[SCN] in an aqueous solution of [C_4mim]Cl induced opposite solubility trends. The addition of Na[$N(CN)_2$] promotes a higher ability to solubilize syringic acid than in the corresponding IL system due to a pH buffering effect, resulting in the deprotonation of the solute. The addition of Na[SCN], on the other hand, induces a relative decrease in syringic acid solubilization at higher concentrations of ILs due to the negative contribution of the NaCl formed by anion-exchange. These results emphasise the often overlooked pH contribution provided by ILs for biomolecule solubilisation whilst providing experimental insights into the structure of aqueous solutions of ionic liquids and the role it plays in the formation of IL-salt aggregates.

Introduction

Although water is listed at the top of the ranking of sustainable solvents, its use in some applications is still considered a great challenge.[1] Despite its extraordinary properties, water can hardly be considered as an optimal solvent due to its poor solvation capability for many molecules of interest.[2,3] This limitation can be overcome with the use of additives, such as surfactants, co-solvents or hydrotropes.[4] Hydrotropes are amphiphilic compounds which interact favorably with both water and hydrophobic molecules.[4,5] They can be either ionic or nonionic, and are used to increase the solubility of hydrophobic solutes in aqueous media.[6] Their small apolar volume prevents the spontaneous self-assembly into organized phases such as the micellar arrangement of surfactants. Even in the presence of a hydrophobic solute, their aggregation does not lead to organized micellar structures due to their small hydrocarbon chains, or apolar regions, resulting in a smaller hydrophobic effect.[7,8]

Historically, the underlying mechanism governing the hydrotropic effect was rationalised by various theories including (i) the self-aggregation of hydrotropes analogous to micellar solubilization,[9–11] (ii) disruption of the "water structure" by the hydrotrope that would behave as a chaotropic agent weakening the hydrophobic effect,[12] and (iii) specific stoichiometric association between a solute and a hydrotrope. These theories cannot be sustained and seem to be at odds with the latest progress in the field. To deepen the analysis of hydrotropy, a thermodynamic model was proposed based on the Kirkwood–Buff (KB) theory,[13] capable of relating properties such as solubility, partial molar volume, and water activity coefficients. The most recent cooperative theory of hydrotropy[14] proposes that hydrotropy is described as the accumulation of hydrotrope molecules around solute molecules, causing the driving force of hydrotropy to be hydrophobic interactions between the hydrotrope and the solute.[15,16] It is important to emphasise that multiple experimental variables can influence a solute's solubility and can be erroneously assigned to a "hydrotropic"

CICECO – Aveiro Institute of Materials, Department of Chemistry, University of Aveiro, 3810-193 Aveiro, Portugal. E-mail: nicolas.schaeffer@ua.pt, jcoutinho@ua.pt

† Electronic supplementary information (ESI) available: Solubility data, pH, regression using the cooperative model, proton chemical shifts ($\Delta\delta_H$) of the systems, normalization area under the curve by Raman spectroscopy for samples, aggregate size distribution by intensity obtained by DLS. See DOI: **https://doi.org/10.1039/d3cp02034g**

effect despite their different mechanisms. One factor of extreme importance in terms of solubility for many biomolecules is the impact of pH. The solubility of ionizable compounds depends on the pH of the solution in which it is being dissolved and is influenced by the interactions between the intermolecular forces.

It has been well established for more than a century that the addition of different salts to water can change the behavior of non-electrolytes in solution.[17–19] In fact, the first study by Carl A. Neuberg to coin the term ''hydrotropism'' to describe the solubilisation of pentanol by salts of aromatic acids is from 1916.[20] Specific ion effects, manifested as the change in solubility of a solute in water upon addition of a salt, are macroscopically described as salting-in or salting-out to indicate the increase or decrease in solubility, respectively.[21] The propensity of a salt to induce either phenomenon is determined by its charge density, polarizability, and volume, and is qualitatively ordered according to the Hofmeister series.[22] Hydrotropy and salting-in can be used to enhance the solubility of poorly soluble compounds in aqueous media, with some ions such as sodium benzoate or 1-methyl-3-butylimidazolium chloride ([C_4mim]Cl) presenting dual effects due to their organic groups.[23] Whilst both contributions can best be rationalised in terms interfacial accumulation or depletion, it is important to emphasise that as fully inorganic anions do not possess hydrophobic moieties (by common definition), their mechanism of action can differ from that of classical hydrotropes.[24–26]

In the last decade, ionic liquids (ILs) were shown to be a promising class of ionic hydrotropes, since both parts of their structure (cationic and anionic) if properly selected, can play an important role to increase the solubility of hydrophobic compounds in aqueous solution.[23,27] The very driving force behind the melting point decrease in ILs, namely the poor intermolecular packing resulting from the introduction of bulky and flexible – typically organic – cations presenting a low charge density, confers ILs the required structural characteristics to act as hydrotropes. In fact, recent studies demonstrated that [C_4mim]-based ILs may perform better than classical ionic hydrotropes,[23,27] especially when combined with anions of increasing apolarity such as thiocyanate ([SCN]$^-$), dicyanamide ([$N(CN)_2$]$^-$) or tosylate ([TOS]$^-$).[28,29] For example, the aqueous solubility enhancement (S/S_0, where S_0 is the solute concentration in pure water) of the drugs naproxen and ibuprofen is one order of magnitude larger using [C_4mim][TOS] rather than the equivalent sodium salt Na[TOS],[29] challenging the common wisdom that ionic hydrotropes require a highly hydrophilic counterion.[6]

Despite their potential, the contribution of certain parameters to the efficacy of ILs as hydrotropes remains unclear including the pH buffering effect, the degree of ''ionicity'' (dissociated ions *versus* ion-pairs),[30] and the evolving nanostructural organization of the mixture into apolar and polar domains at higher IL concentrations.[31] As for surfactant micellization, where the size and shape of the resulting aggregate depend on the interfacial accumulation of ions as per the Hofmeister series,[32] the solute mediated aggregation of ionic hydrotropes is stabilised by some degree of counter-anion binding and therefore ionicity.[29] The size of the resulting aggregate is contingent on the local charge, with a compromise required between favourable ion-pairing, which positively influences the apolarity and total contributing hydrotrope volume, and minimizing conditions for which pre-structuration of the liquid phase promotes hydrotrope–hydrotrope interactions. In a previous study, we showed that chloride salts in the presence of [C_4mim]Cl promote a more pronounced decrease in the solubility of aromatic biomolecules compared to the corresponding system without a hydrotrope.[33] This effect was found to be dependent both on the IL concentration and salt valency and was attributed to the competing interaction between intermolecular IL interactions at higher salt concentrations at the expense of solute–hydrotrope interactions.

This work aims to extend our previous study in light of the enumerated problematics by studying the impact of sodium salt anions on the hydrotropic dissolution of syringic acid using [C_4mim]Cl as a hydrotrope, with a focus on the dicyanamide Na[$N(CN)_2$] and thiocyanate Na[SCN] salts. The final solution pH was systematically recorded to decorrelate pH from hydrotropy contributions on the total solubility, whilst the cyano-band of the salt anions is sensitive to the local environment, allowing us to probe the degree of anion-exchange and ion-pair formation *via* Raman spectroscopy. Additional techniques including dynamic light scattering (DLS) and 1D proton nuclear magnetic resonance spectroscopy (NMR) were employed to gain an understanding of hydrotrope–solute interactions and establish their variation as a function of the solution ionic strength. The obtained results shed light on the site specific interactions between the hydrotrope and solute that are lost at higher ionic strengths, pH effect from the anion, and the negative salting-out contribution of the NaCl formed *in situ*.

Experimental

Chemicals

The ionic liquids 1-butyl-3-methylimidazolium ([C_4mim]Cl, 99.0 wt%), 1-butyl-3-methylimidazolium thiocyanate ([C_4mim][SCN], 99.0 wt%) and 1-butyl-3-methylimidazolium dicyanamide ([C_4mim][$N(CN)_2$], 99.0 wt%) were purchased from IoLiTec. The solute under investigatation is syringic acid (97.0 wt%), obtained from Acros Organics. The following salts were procured from various suppliers: sodium dicyanamide (Na[$N(CN)_2$], 96.0 wt%) from Alfa Aesar, sodium thiocyanate (Na[SCN], 98.0 wt%) from Sigma-Aldrich, sodium sulfate (Na_2SO_4, 99.99 wt%) from Sigma-Aldrich, sodium chloride (NaCl, 99.5 wt%) from Fisher Scientific, sodium tosylate (Na[TOS], 90.0 wt%) from TCI, and sodium nitrate (Na[NO_3], pure) from Honeywell. All chemicals were used as received without further purification. Ultrapure, double distilled water passed through a reverse osmosis system and was further treated with a Milli-Q plus 185 water purification apparatus (18.2 MΩ cm at 25 °C) and was used for all experiments.

Solubility measurements

The solubility of the syringic acid in the hydrotropic systems studied was experimentally determined using an isothermal

shake-flask method, previously described in the literature.[27,34] The systems, water/hydrotrope/salt solutions were prepared in the range of concentrations of (0 at 80 wt%) of hydrotrope in water and for three fixed salt concentrations of 0.5 mol L^{-1}, 1.0 mol L^{-1} and 2.0 mol L^{-1}. The samples were allowed to equilibrate under constant agitation (1050 rpm) at 303.2 ± 0.5 K and an equilibrium time of 72 h using an Eppendorf Thermomixer Comfort apparatus and excess syringic acid was added to these samples to keep all solutions saturated to equilibrium. All solubility tests were performed in triplicate. After equilibration (72 h), all samples were left ''overnight'' and were subsequently subjected to filtration and centrifugation in a Hettich Mikro 120 centrifuge at 4500 rpm and a temperature of (303.2 ± 0.5) K for 20 minutes, in order to guarantee the separation of the undissolved solute from the liquid phase. The syringic acid concentration in the liquid phase was quantified *via* UV spectroscopy using a SHIMADZU UV-1700, Pharma-Spec spectrometer at a wavelength of 267 nm in a quartz-cell cuvette with a path length of 1 cm. A previously established calibration curve was used after validation (absorbance = [syringic acid concentration] × 44.55; calibration performed for syringic acid concentrations between 0.001 and 0.020 g L^{-1}).[29] To avoid interference from the imidazolium cation absorption peak at 211 nm, samples of the liquid phase were carefully collected and appropriately diluted by a minimum factor of 2000 prior to quantification. Additionally, the absorbance of an aqueous solution with an equivalent [C_4mim]Cl concentration was subtracted from the sample spectra to control for the IL during syringic acid quantification. An identical protocol was followed to determine the solubility of syringic acid in inorganic salt and water solutions.

The final solution pH of all studied hydrotrope systems, either hydrotrope + solute or hydrotrope + solute + salt, was measured using a Mettler Toledo SevenExcellence pH meter. After calibration, according to manufacturer instructions, the electrode was inserted in a sample for at least 2 minutes. After this period, the pH was measured in triplicate at room temperature (~295 K). The uncertainty on the pH values presented is ±0.02. All measurements were performed within a period of 24 h after solute saturation was achieved according to the solubility measurement procedure described previously. Due to the large number of systems studied, the final pH value was only recorded for systems containing a fixed hydrotrope concentration of 2.0 mol L^{-1}.

Solubility measurement analysis

Setschenow constant. An important parameter in the context of solubility studies is the relative effectiveness of salting-out or salting-in traditionally quantified by the use of the Setschenow constant.[35] The Setschenow constant is proposed as a practical approach to describe the effect of a salt or additive on the solubility of a compound in an aqueous solution.[36] Therefore, this constant was here adapted to quantify the change in solute solubility due to the presence of an IL + salt. It is herein defined as:

$$\ln S_s = K_H \cdot C_S \quad (1)$$

$$K_H = \sum K_i x_i \quad (2)$$

where S_s is the molar solubility of the solute, K_H is the system Setschenow constant, C_s is the molarity of the hydrotropic system and K_i is the Setschenow constant in the ternary system of water + solute + compound i. Eqn (1) is valid from the hydrotropic molarity of zero up to a value in which the change in the natural logarithm of solute solubility remains linear with increasing molarity of the system. The Setschenow constant adapted for each IL + solute + salt + water was obtained from linear least square regressions of the logarithm (S/S_0) and C_s for a variable IL concentration at a fixed salt concentration, essentially treating the system as pseudo ternary one. K_H will be positive when salting-in occurs and negative when salting-out takes place. It is important to bear in mind that the Setschenow constant defined as per eqn (1) is not an empirical equation but is linked to the Kirkwood–Buff integrals (KBIs) in the following manner:

$$K_H \propto G_{S,H} - G_{S,W} \quad (3)$$

where $G_{S,H}$ is the KBI between the solute and the hydrotrope, and $G_{S,W}$ is the KBI between the solute and water.

Cooperative hydrotropy model. Shimizu and Matubayasi[14] developed a statistical thermodynamics-based model (henceforth named cooperative hydrotropy model) to describe hydrotropy. The model can be expressed in the following manner:

$$\frac{S}{S_0} = \frac{1 + e^b \left(\frac{S}{S_0}\right)_{max} x_H^m}{1 + e^b x_H^m} \quad (4)$$

or in the linearized form from which model parameters m and b can be obtained by linear regression:

$$\ln\left[\frac{1 - \frac{S}{S_0}}{\frac{S}{S_0} - \left(\frac{S}{S_0}\right)_{max}}\right] = m \ln(x_H) + b \quad (5)$$

where S_0 is its molar solubility in water, $(S/S_0)_{max}$ is the maximum attainable relative solubility, and x_H is the mole fraction of the hydrotrope (in the hydrotropic system and not on a solute-free basis). Finally, m and b are parameters of the model, both with a physical meaning described in the Discussion section.

Hydrotrope–solute interactions

Nuclear magnetic resonance (NMR) spectroscopy. Selected samples were prepared and analyzed using one-dimensional proton NMR spectra to provide information regarding the chemical environment of the IL and syringic acid mediated by the addition of salts and the possible hydrotrope/solute interactions. ^{1}H-NMR measurements were performed on a Bruker Avance 300 NMR spectrometer operating at 300.13 MHz, at 293.15 K. The samples were inserted into a glass NMR tube with a sealed capillary added to a coaxial insert containing D_2O and trimethylsilylpropanoic acid (TSP, 98 mol% D atoms) as an internal standard.

Dynamic light scattering (DLS) analyses. To verify the formation of aggregates, DLS analyses were performed using a Zetasizer Nano-ZS photometer from Malvern Instruments. The samples were filtered through a 0.45 μm nylon syringe and then left in an ultrasonic bath for 5 minutes to promote the dispersion and degassing of the particles. DLS analyses were performed at 293.15 K, with an equilibration time of 120 seconds. Irradiation was performed at a wavelength of 565 nm using a helium–neon laser and the scattered light was detected at a backscattering angle of 173°. The automatic mode was used for the measurements and data processing and was corrected for the viscosity (1.315 and 1.730 mPa s) and refractive index (1.348 and 1.366) of both IL 0.5 mol L^{-1} and 1.5 mol L^{-1} aqueous solutions, respectively. The analyses were performed in triplicate and the extracted results are averages.

Raman spectroscopy. The Raman spectra were obtained with a resolution of 4 cm^{-1} in the spectral range 0–3800 cm^{-1} on a Horiba Jobin-Yvon XploRA spectrometer in a back-scattering geometry after collecting for 20 s and accumulated 60 times. The Gaussian curves were fitted using commercially available software (OriginLabR corporation) to identify peak positions and intensities. Quantitative analysis of the area integrals and derivatives of the fitted curves were then used to calculate the integrated intensity *vs.* area ratio.

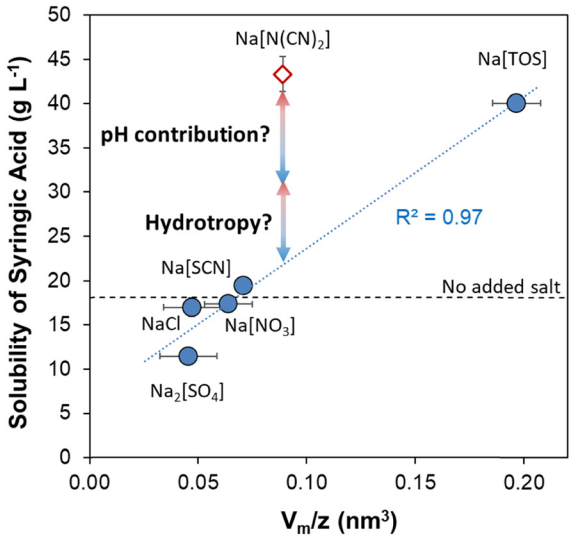

Fig. 1 Solubility of syringic acid in an aqueous solution of 1.0 mol L^{-1} of $[C_4mim]Cl$ with 1.0 mol L^{-1} of sodium salts as a function of the charge density of the sodium salt anion expressed as the molecular volume (V_m) divided by its charge (z). The blue and red symbols correspond to experiments where the final solution pH was respectively below and above the pK_a of syringic acid (pK_a = 4.20).[43] All solubility data are available in Table S1 (ESI†). The error bars (y-axis) represent the standard deviation from three independent measurements. All measurements were performed at T = 303.2 K.

Results and discussion

Anion contribution and pH effect

In the majority of studies on salting-in or salting-out effects, the anion has a much larger impact than the cation and the ordering of anions in terms of salting power often follows the Hofmeister series.[17,37] In this first section, sodium salts with varying anions from $Na_2[SO_4]$ to $Na[N(CN)_2]$ were investigated as additives, syringic acid was chosen as the solute and the ionic liquid $[C_4mim]Cl$ as the hydrotrope. The solubility of syringic acid in the presence of sodium salts and IL was measured at a fixed concentration of 1.0 mol L^{-1} for each, respectively. Each data point is an average of 3 independent measurements. The low coefficients of variation, less than 5%, indicate that the standard deviations are much smaller than the solubility values. These results are described in Fig. 1 and the relevant properties of the system components are summarised in Table 1.

Table 1 Molecular volume (V_m) and Gibbs free energy of hydration (ΔG_{HYD}) of the compounds studied in this work

Compound	V_m (nm^3)	ΔG_{HYD} (kJ mol^{-1})
Na^+	0.004[a]	−365[d]
$[C_4mim]^+$	0.196 ± 0.021[b]	—
$[SO_4]^{2-}$	0.091 ± 0.013[a]	−1080[d]
Cl^-	0.047 ± 0.013[a]	−340[d]
$[NO_3]^-$	0.064 ± 0.011[a]	−300[d]
$[SCN]^-$	0.071 ± 0.003[a]	−280[d]
$[N(CN)_2]^-$	0.089 ± 0.010[b]	−255[e]
$[TOS]^-$	0.197[c]	−305[e]
Syringic acid	0.222[c]	—

[a] Taken from ref. 38. [b] Taken from ref. 39 [c] Derived from crystal structures (CCDC Database identification number 1450484 and 116426). [d] Taken from ref. 40. [e] Taken from ref. 29.

The introduction of the IL into an aqueous solution raises the solubility of syringic acid from 1.48 g L^{-1} to 18.08 g L^{-1} (no pH control), resulting in an S/S_0 of 12.21 and confirming the excellent performance of the $[C_4mim]^+$ cation as a hydrotrope. Following the Hofmeister series, in which the salting-in/out potential of the anions proceeds according to $[SO_4]^{2-} < Cl^- < [NO_3]^- < [SCN]^- < [N(CN)_2]^- \sim [TOS]^-$, the presence of the highly solvated $[SO_4]^{2-}$ induces a decrease in the ability of the system to solubilize syringic acid (11.43 g L^{-1}). Correspondingly, anions to the right of $[Cl]^-$ promote the solubilisation of syringic acid as observed in $[SCN]^-$ (19.38 g L^{-1}), $[TOS]^-$ (40.06 g L^{-1}), and $[N(CN)_2]^-$ (43.32 g L^{-1}), inducing a salting-in effect. Note that in the quaternary system under study (excluding water) comprising the solute, $[C_4mim]^+$, Cl^-, Na^+ and its counteranion, approximately quantitative anion exchange between the IL and sodium salt is anticipated for anions to the right of chloride along the Hofmeister series.[41] For such systems under equimolar conditions, it is more accurate to consider the components as $[C_4mim][X]$, where [X] = $[NO_3]^-$, $[SCN]^-$, $[TOS]^-$ or $[N(CN)_2]^-$, and NaCl as a weak salting-out agent[42] due to the *in situ* formation of a different IL. The presence and influence of NaCl are best represented by the lower solubility of syringic acid in the IL + salt system containing NaCl and $Na[NO_3]$ which present a lower solubility

than the IL + water system (18.08 g L^{-1}). Similarly, an investigation of the system comprising [C_4mim]Cl, vanillin as a solute, and NaCl as an added electrolyte also identified a small salting-out effect of NaCl compared to the binary IL + solute system.[33] The decreased solubility of vanillin was assigned to the increased self-aggregation of the IL in the presence of salt at the expense of solute–hydrotrope interactions.

When attempting to correlate the influence of salt on syringic acid solubility as a function of the anion properties in the absence of pH control, significant positive divergences were observed for systems with the $[N(CN)_2]^-$ anion as shown by the red symbols in Fig. 1 compared to the other salt systems. Whilst improved solute solubility could be anticipated in the case of $[TOS]^-$ due to its larger volume and organic nature compared to the other anions, making it a known anionic hydrotrope,[44] the two-fold increase in syringic acid solubility when changing from $[SCN]^-$ to $[N(CN)_2]^-$ is unexpected. Measurements of the final solution pH for all systems, with the exception of the aforementioned $[N(CN)_2]^-$ anion, were in the range of 3.18 to 3.54 (see Table 3 further on). These values are below the pK_a of of syringic acid (pK_a = 4.20) such that the neutral form of syringic acid dominates.[43] In contrast, the greater basicity of the $[N(CN)_2]^-$ anion is reflected in a final pH value of 5.30, signifying that both pH effects and hydrotropy contribute towards the sudden increase in the solubility of syringic acid. The ionisation of molecular species is a well-established approach to improve the low-water solubility of biomolecules, with the aqueous solubility of sodium syringate (10.33 ± 0.56 g L^{-1}, determined in this work) and cholinium syringate (553.7 ± 3.37 g L^{-1}) being approximately 10 and 550 times greater than for syringic acid, for example.[45] Unfortunately, the instability of dicyanamide under acidic conditions, leading to its decomposition with the release of heat and toxic gases, prevents us from conducting a similar study as shown in Fig. 1, with pH control to accommodate the varying basicity of the studied anions.[46]

To summarise, the influence of the salt anion on the total solubility of syringic acid approximately follows the Hofmeister series if the solution pH and increased solubility of sodium syringate are considered. Nevertheless, pH contributions must be explicitely considered to explain the experimental variability, with the pH effect being non-linear and dependent on the IL concentration. The following sections will focus on two systems with structurally similar salts, namely Na[SCN] and Na[$N(CN)_2$], but presenting differing solubility trends to better understand the delicate balance among pH, hydrotropy, and the Hofmeister effect on the solubilisation process.

Ternary hydrotrope–solute–water system

The presented results will be introduced in order of system complexity to better appreciate the contribution of each component, focusing first on the ternary IL + solute + water system before considering the effect of added salts and their potential pH effect. The behavior of the hydrotropes [C_4mim]Cl, [C_4mim][SCN] and [C_4mim][$N(CN)_2$] in aqueous solutions and their ability to enhance the solubility of syringic acid is presented in the absence of pH control. The solubilities were measured over the entire experimentally available concentration range of the hydrotrope, from pure water to the limit of aqueous solubility. The resulting solubility curves are shown in Fig. 2A, along with the fitted curves of the cooperative hydrotropy model (in the ESI,† Fig. S1) in Fig. 2B. Additionally, the same solubility data were represented as moles of solutes per mole of IL (solute free basis) in the system at equilibrium, as shown in Fig. 2C. This triptic representation permits an assessment of the solubility data as a function of the desired objective, namely maximizing the total solute solubility or identification of the most "efficient" hydrotrope on a molar basis. The final solution pH in each system was measured for IL concentrations of 60 wt%.

Fig. 2A shows an approximately 80-fold increase in the aqueous solubility of syringic acid using [C_4mim]Cl or [C_4mim][SCN] as hydrotropes, obtained at concentrations of 60 and 70 wt%, respectively; under such conditions, water is no longer the main solvent in terms of mass. In contrast, [C_4mim][$N(CN)_2$] promotes a more efficient solubilisation of syringic acid at lower hydrotrope concentrations despite exhibiting a smaller maximum solubility enhancement of S_{max}/S_0 = 36

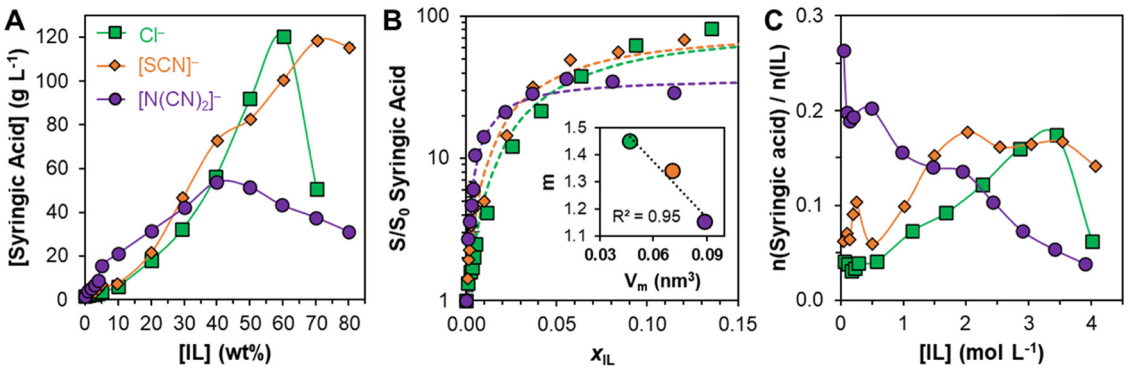

Fig. 2 (A) Total aqueous solubility, (B) solubility enhancement (S/S_0) along with the fitted curve (dashed line) obtained using the cooperative hydrotropy model, and (C) moles of solute per mole of the hydrotrope for syringic acid as a function of the concentration (solute-free basis) of [C_4mim]Cl (■), [C_4mim][SCN] (◆) and [C_4mim][$N(CN)_2$] (●) at T = 303.2 K. Full lines are visual guides. The inset in panel (B) shows the parameter m of the cooperative hydrotropy model for the ILs as a function of the anion volume. All solubility data are available in Tables S2–S4 (ESI†).

for 40 wt% IL. The existence of a solubility maxima in a ternary system greater than that of the individual pure compounds is in itself not unconmon and was previously reported for a range of solute/hydrotrope combinations including for the solubility of two antioxidants (gallic acid and vanillin) by aqueous solutions of [C_4mim]Cl.[47]

The underlying driving force for the hydrotropy model of Shimizu and Matubayasi[14] is the aggregation of hydrotrope molecules around the solute, expressed as the difference in the KBIs between $G_{S,H}$ and $G_{S,W}$. Any modifications in the solution composition, either through a change in the hydrotrope concentration or through the introduction of inorganic salts, that reduces the magnitude of this term will negatively impact the efficacy of a given hydrotrope.[33] From this definition, the efficiency of a hydrotropy system, in which the hydrotrope is ionic, is better estimated under dilute conditions where the hydrotrope can be considered as fully dissociated ions. The change in the proportion of dissociated to ion-pairs and the emergence of a solute-independent structuration of the liquid phase into nano-seggregated polar and apolar domains with the increase in IL concentration will impact the total solubility.[48]

Whilst no structured aggregates were detected for aqueous [C_4mim]Cl solutions in the absence of a solute, conductivity and surface tension experiments identified a gradual change in the system properties above approximately 1.0 mol L^{-1}.[49–51] Furthermore, a clear liquid phase seggregation of the alkyl-domain was evidenced by molecular dynamics simulated small-angle X-ray scattering of a 3.5 mol L^{-1} solution of [C_4mim]Cl,[52] the same IL concentration corresponding to the maximum of S/S_0 shown in Fig. 2. The evolution from an isotropic liquid solution to one presenting spatial organization at the nano-scale presents potentially differing solubility mechanisms. A compromise therefore emerges with the increase in IL concentration between the factors controlling the solubility of syringic acid, namely the pre-existence of apolar domains (favourable) and the energy for solvent restructuring in the presence of a solute (unfavourable). The choice of the IL anion is likely to particularly impact the former factor due to the change in the degree of counter-ion binding for a given IL concentration.[53] To clarify, although we make mention of aggregates and domains, these are in dynamic equilibrium and represent statistical approximation of the system over a given duration.

The improved hydrotropic capacity of [C_4mim][$N(CN)_2$] under ''dilute'' conditions is reflected in Fig. 2C in which an approximately linear decrease in the moles of solute per mole of hydrotrope is observed with increasing [C_4mim][$N(CN)_2$] concentration. In contrast, the n(solute)/n(hydrotrope) ratio sharply increases for initial [C_4mim]Cl concentrations of 1.0 mol L^{-1} and increases linearly until reaching a maximum at 3.5 mol L^{-1}. A similar profile is obtained for [C_4mim][SCN], albeit with a maximal plateau concentration range from 1.5 mol L^{-1} onwards, rather than a clear maximum solubility composition as in the case of [C_4mim]Cl. To what extent the differing behaviour of [C_4mim][$N(CN)_2$] is attributable to a pH effect will be addressed in the next section. Application of the cooperative hydrotropy model to the dilute region, *i.e.* [IL] < 50 wt%, results in the solubilisation curves presented in Fig. 2B from which the model parameters m and b were extracted. The parameter m corresponds to the number of hydrotrope molecules involved in the solvation of the solute and b is related to the ease of inserting that number of hydrotrope molecules in the volume corresponding to the vicinity of the solute. The evolution of m as a function of the IL anion volume, as shown in the inset of Fig. 2B, suggests that the greater molecular efficiency of [C_4mim][$N(CN)_2$] in the diluted region is due to its larger total volume (V_m(IL) = V_m(cation) + V_m(anion)). This large volume enables it to effectively hydrate a greater surface area of solute per mole of hydrotrope. A large discrepency is observed between the obtained m values shown in Fig. 2B and the molar ratio of the solute to hydrotrope shown in Fig. 2C, suggesting that most hydrotrope molecules do not directly contact the solute. This discrepancy is attributed to the excessive aggregation of the hydrotrope due to hydrophobic hydrotrope–hydrotrope interactions rather than solute–hydrotrope interactions, the former being exacerbated by the increased solution ionic strength. A more detailed discussion of the mechanism contributing to the solubilisation mechanism in the systems containing Na[SCN] and Na[$N(CN)_2$] is presented further on.

Hydrotropy in the presence of salts

The previous sections reconciled the relationship between the effect of anions, hydrotrope concentration, and pH on the solubility of syringic acid at a given concentration. In this section, the additive solubility curves approach are explored to provide more information on how the salts interact with the solute/hydrotrope and to validate the hypothesis drawn above. Syringic acid was maintained as the solute and the ionic liquid [C_4mim]Cl as the hydrotrope to evaluate the impact of Na[$N(CN)_2$] and Na[SCN] at three different molar concentrations of salt (0.5, 1.0 and 2.0 mol L^{-1}). The solubility curves of syringic acid in aqueous solutions of ILs and the mentioned sodium salts were determined and are shown in Fig. 3A, B and 4A, B. All solubility data are available in Tables S2–S4 (ESI†).

The relative solubility was calculated according to eqn (6) to better represent the synergistic or antagonistic solubility change upon salt addition:

$$S = \frac{S_{mix}}{\left(S_{0_{IL}} + S_{0_{Salt}}\right)} \quad (6)$$

where S represents the relative solubility of syringic acid, S_{mix} is the solubility of syringic acid in (mol kg^{-1}) in the mixture of water + IL + salt, and $S_{0_{IL}}$ and $S_{0_{salt}}$ represent the solute solubility in the systems of water + IL and water + NaX (X = [$N(CN)_2$] or [SCN]), respectively, for a fixed IL or sodium salt concentration. The initial syringic acid solubility values (S_0) in water and aqueous salt solutions are presented in Table 2. It is worth highighting that these are complex multi-component solutions and that the above notation is a simplification. When considering ion-dissociation, the systems of H_2O + IL or H_2O + NaX could be considered as ternary systems whilst H_2O + IL + NaX a

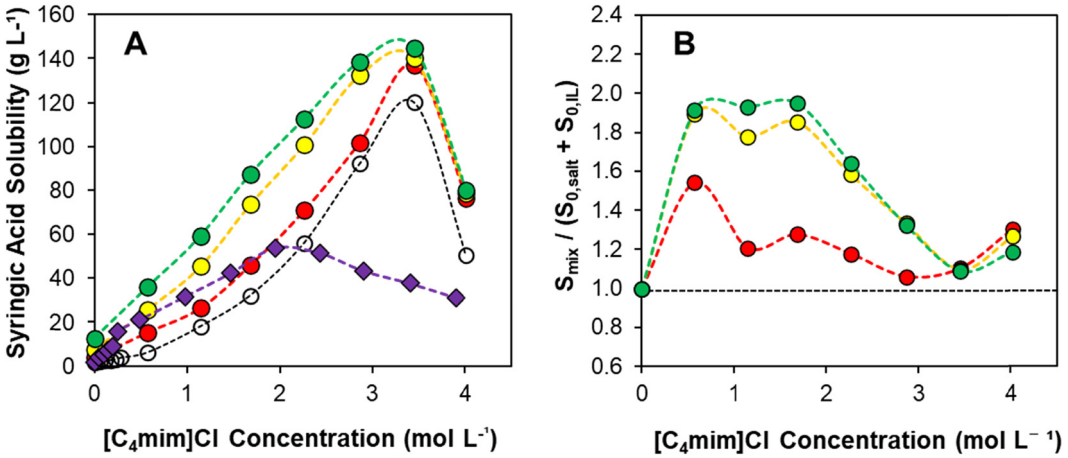

Fig. 3 (A) Aqueous syringic acid solubility in aqueous [C_4mim]Cl solution in the presence of individual salt Na[N(CN)$_2$] at concentrations of 0.5 ●, 1.0 ●, 2.0 mol L^{-1} ● and ◆ [C_4mim][N(CN)$_2$] at T = 303.2 K. (B) $S_{mix}/(S_{0\ IL} + S_{0\ salt})$ is the relative solubility of syringic acid as a function of hydrotrope concentration. The dashed lines are visual guides. The final pH values of the systems containing 2.0 mol L^{-1} IL increase from 4.80 to 6.12 for 0.5 to 2.0 mol L^{-1} Na[N(CN)$_2$], respectively.

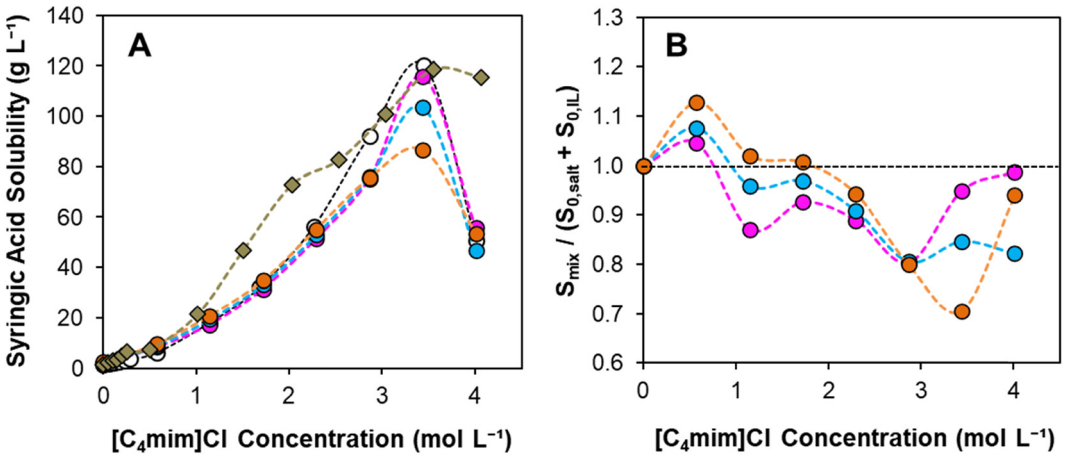

Fig. 4 (A) Aqueous syringic acid solubility in aqueous [C_4mim]Cl solution in the presence of individual salt Na[SCN] 0.5 ●, 1.0 ● 2.0 mol L^{-1} ● and ◆ [C_4mim][SCN] at T = 303.2 K. (B) $S/(S_{0mix} + S_{IL})$ is the relative solubility of syringic acid as a function of hydrotrope concentration. The dashed lines are visual guides. The final pH values of the systems containing 2.0 mol L^{-1} IL range from 3.54 to 3.71 for 0.5 to 2.0 mol L^{-1} Na[SCN], respectively.

Table 2 Solubility and associated standard deviation of syringic acid in water aqueous solutions of the studied salts at 303.2 K

Compounds	[Salt] (mol L^{-1})	S_0 (g L^{-1})	Error
Water	—	1.48	0.08
Na[N(CN)$_2$]	0.5	3.87	0.01
	1.0	7.50	0.02
	2.0	12.63	0.01
Na[SCN]	0.5	1.82	0.01
	1.0	2.14	0.02
	2.0	2.42	0.10

quintenary one. Nevertheless, eqn (6) allows us to implicitely consider the salt pH effect through the value of $S_{0,Salt}$, thereby providing a clearer insight into the relative contribution of hydrotropy and pH to the total solubility. Finally, the final system pH values at equilibrium for a fixed hydrotrope concentration of 2.0 mol L^{-1} were systematically recorded and are available in Table 3 for a better appreciation of the differing pH contribution (the pK_a of of syringic acid is 4.20).

The results show that, as expected, both salts act as medium to strong salting-in inducers. At 2.0 mol L^{-1}, Na[N(CN)$_2$] is able to enhance the solubility of syringic acid by almost one order of magnitude due to its buffering influence on the pH (pH = 6.25 at solute saturation, Table 3). In Fig. 3A, the solubility of syringic acid in aqueous [C_4mim]Cl solutions consistently increased in the presence of Na[N(CN)$_2$] for all concentrations. A synergistic mechanism is obtained here, in which the ternary mixture of solvents (around pH 4.80–6.12 at solute saturation, Table 3) exhibits a higher solubility of syringic acid than that achieved by the combined individual effects. Although this

Table 3 Setschenow constants (K_H), cooperative hydrotropy constants (m and b), and final pH values at solute saturation for syringic acid in the hydrotrope systems studied in this work (T = 303.2 K). The final solution pH was measured at a fixed hydrotrope concentration of 2.0 mol L^{-1}

Mixture	[Salt] (mol L^{-1})	K_H	Error	C_s	M	b	pH
$[C_4mim]Cl$	—	0.102[a]	0.00	0.0–2.0	1.45	3.81	3.23
$[C_4mim][N(CN)_2]$	—	0.143[a]	0.01	0.0–2.0	1.15	4.77	6.25
$[C_4mim][SCN]$	—	0.070[a]	0.00	0.0–2.0	1.34	3.85	3.54
$[C_4mim][TOS]$	—	0.158[a]	0.001	0.0–2.0	1.17	4.79	3.45
$Na[N(CN)_2]$	—	0.028[a]	0.01	0.0–2.0	—	—	5.35
$Na[SCN]$	—	0.002[a]	0.01	0.0–2.0	—	—	3.18
NaCl	—	−0.612[a]	0.01	0.0–2.0	—	—	3.09
$[C_4mim]Cl$ + $Na[N(CN)_2]$	0.5	0.183	0.01	0.0–2.0	1.56	4.40	4.80
	1.0	0.235	0.01	0.0–2.0	2.01	6.70	5.30
	2.0	0.258	0.01	0.0–2.0	1.97	6.55	6.12
$[C_4mim]Cl$ + $Na[SCN]$	0.5	0.101	0.02	0.0–2.0	1.59	4.13	3.54
	1.0	0.107	0.01	0.0–2.0	1.64	4.49	3.54
	2.0	0.111	0.01	0.0–2.0	1.87	5.42	3.71

[a] K_i is the Setschenow constant of compound (i) in a single electrolyte solution.

evidence is present across the concentration range of the IL + salt mixtures studied, it can be observed more clearly at lower concentrations of the IL, disappearing at the higher concentrations as shown in Fig. 3B. As the salt concentration is increased, a synergistic salting-in effect dominates the system, and an up to 2-fold increase in solubility above the individual effects of the salt and the IL is achieved at 2.0 mol L^{-1} of $Na[N(CN)_2]$ concentration. Interestingly, the general shape of the curve and its maximum peak solubility do not vary with the salt concentration used, being independent of the ionic strength and anion exchange under the conditions tested, remaining in the region of 3.5 mol L^{-1} of IL. This allows new ''puzzles'' and combinations to be made for these hydrotropic systems. For example, assuming complete anion exchange for each mole of $Na[N(CN)_2]$ added, the solubility of the $[C_4mim]Cl$ + $Na[N(CN)_2]$ system for $Na[N(CN)_2] \geq 1.0$ mol L^{-1} exceeds that of $[C_4mim][N(CN)_2]$ at the same IL concentration. The observed reversal in the curve behavior of these mixtures (hydrotrope/additive) above the maximum in the solubility of syringic acid must be related to a change in the molecular mechanism of solvation in these regions as previously discussed elsewhere.[54]

The effect of another salting-in sodium salt, Na[SCN], was also investigated. Its effect on the solubility of syringic acid is less important than $Na[N(CN)_2]$ as reported in Table 2, and the results related to the effect of the hydrotropic dissolution are shown in Fig. 4A and B. Contrary to what was observed for $Na[N(CN)_2]$, this salt seems to induce a somewhat antagonistic effect by decreasing the solubility of syringic acid when compared with the aqueous solutions of the individual compounds, as highlighted in Fig. 4B.

Therefore, it is necessary to investigate in more detail which mechanism is dominant in these systems. An important parameter in the context of solubility studies is the relative effectiveness of salting-out or -in, traditionally quantified by the use of the Setschenow constants. The Setschenow constant adapted for each IL + solute + salt was obtained from linear least squares regression fittings of the logarithm (S/S_0) and C_s for both concentrations of the systems obtained in Table 3. K_H will be positive when salting-in occurs and negative when salting-out occurs.

According to the results in Table 3, there is a gradual increase in the Setschenow constants with the salt concentration of $Na[N(CN)_2]$ and Na[SCN]. The individual constant of each component of the mixture confirms the existence of a synergistic effect between the components of the $[C_4mim]Cl$ + $Na[N(CN)_2]$ system, where the sum of the individual components (K_i) is smaller than the K_H obtained for the mixed system. The Setschenow analysis suggests that the salt concentration exerts an influence on the solubility of these systems, especially in regions of low hydrotrope concentration. Above a certain hydrotrope concentration, the adverse effect prevails on hydrotrope–solute interactions, leading to a negative impact on solubility. In contrast, the K_i results of $[C_4min]Cl$ and Na[SCN] and K_H of the mixture (IL + salt) are essentially constant across the tested salt concentration. This may also be linked to the deleterious effect of the *in situ* formation of NaCl, assuming complete anion-exchange, and its salting-out capacity as established in Table 3. The latter is overcome in the $Na[N(CN)_2]$ system due to the pH effect as evidenced in Table 3.

Further differences are apparent when considering the m values of the cooperative hydrotropy model, with the regression fittings available in Fig. S2 and S3 (ESI†). Whilst a proportional increase of m with Na[SCN] concentration is observed in the quaternary system from 1.34 to 1.87 for Na[SCN] concentrations from 0.0 to 2.0 mol L^{-1}, respectively, no appreciable changes are recorded in $Na[N(CN_2)]$ above 1.0 mol L^{-1}. In the latter system, the m values in the presence of $Na[N(CN_2)] \geq$ 1.0 mol L^{-1} are approximately twice that when using the $[C_4mim][N(CN)_2]$ IL. Based on the previous discussion in the ternary system, an increase in m values suggests a lower atomistic efficiency of the hydrotrope to solubilise the solute. However, this argument is not consistent with the improved solubility of syringic acid in the system of $[C_4mim]Cl$ + $Na[N(CN)_2] \geq 1.0$ mol L^{-1} relative to $[C_4mim][N(CN)_2]$ in spite of the deleterious presence of the formed NaCl in the former. Furthermore, similar m values were obtained for $[C_4mim]Cl$ + 2.0 mol L^{-1} Na[SCN], thereby limiting the possible correlation of the cooperative hydrotropy model variables with the obtained results. As such, a more systematic study of solute–hydrotrope interactions was carried out using other techniques.

Understanding the solute–hydrotrope interactions in the presence of salt

To complement the macroscopic solubility curves reported in Fig. 3 and 4, we further investigated the molecular interactions responsible for this solubility enhancement through NMR, DLS, and RAMAN spectra of the cyano band of the salt anions. From the NMR spectra, it was possible to observe the ^{1}H-NMR displacement ($\Delta\delta_H$) for a quaternary system (IL + salt+ syringic acid) in relation to the same ternary system (IL + solute). ^{1}H-NMR shifts for the IL and syringic acid are available in

Table S5 of the ESI.† Fig. 5A shows the difference between the chemical shifts for the binary system in aqueous IL solution [C_4mim]Cl at a concentration of 1.0 mol L^{-1} saturated with syringic acid and the binary system without any addition of syringic acid and Fig. 5B presents the respective correlation for the solute.

The main goal of this analysis is to provide quantitative insight through the distinct $\Delta\delta_H$ values for each proton. Increased proton shielding was observed for all protons, albeit with different magnitudes. Differences can be observed by changing the aromatic ring of the IL. In cases where lower $\Delta\delta_H$ chemical shifts were retained upon the addition of syringic acid, there is evidence of continued hydration, providing greater protection for the hydrogens in solution, suggesting a greater interaction between the tail part of the hydrotrope and the solute compared to the aromatic ring. The greater $\Delta\delta_H$ associated with the first CH_2 of the cationic butyl chain most likely reflects the change in the electron density on the imidazolium ring and hints at possible additional π–π interactions between the hydrotrope and solute. The same approach was performed for saturated syringic acid (Fig. 5B) dissolved in 1.0 mol L^{-1} IL in an aqueous solution. The chemical structure of syringic acid consists of a single aromatic ring attached to two OCH_3 groups, an OH group and a COOH group. The shielding is most pronounced for the aromatic hydrogens (H4) and (H5). In contrast, for the two methoxy parts attached to the aromatic ring (H1) and (H2), smaller $\Delta\delta_H$ values are observed, suggesting a lower solute–hydrotrope interaction and greater hydration of these groups. The $\Delta\delta_H$ values shown in Fig. 5B suggest that the significant increase in solubility of syringic acid in 1.0 mol L^{-1} IL solutions happens due to the displacement of water molecules around the aromatic ring of the solute, thus revealing strong hydrotrope–solute interactions. This can be observed with more incidence in the analysis of aggregate formation, as measured by DLS discussed later. This experimental evidence is in agreement with the results proposed in our previous study on the effect of chloride salts on vanillin solubility using [C_4min]Cl as a hydrotrope.[23] The results in the ternary system are consistent with the hydrotropy theory proposed by Shimizu *et al.*,[17] in which the hydrotropic solubilization mechanism is driven by the aggregation of hydrotrope molecules surrounded by the solute, while the polar portions are kept in contact with water.

Having determined the site-specific interactions between the hydrotrope and solute in the ternary system without added salt, the influence of $Na[N(CN)_2]$ and Na[SCN] on this system is now determined. Fig. 6A and B shows the difference between the chemical shifts for the quaternary system in aqueous IL solution ([C_4mim]Cl) at a concentration of 1.0 mol L^{-1} and the concentration of salts $Na[N(CN)_2]$ and Na[SCN] (0.5, 1.0 and 2.0 mol L^{-1}) saturated in syringic acid compared to the ternary system (IL + salt) at the same concentration without any addition of syringic acid. All NMR shifts are available in Table S6 (ESI†). Upon comparison, the relative shifts of each imidazolium proton in the $Na[N(CN)_2]$ system (Fig. 6A) present an essentially salt-independent behavior upon introduction of the solute. Furthermore, a similar magnitude of the ring and butyl tail $\Delta\delta_H$ is observable, contrary to the prevailing notion

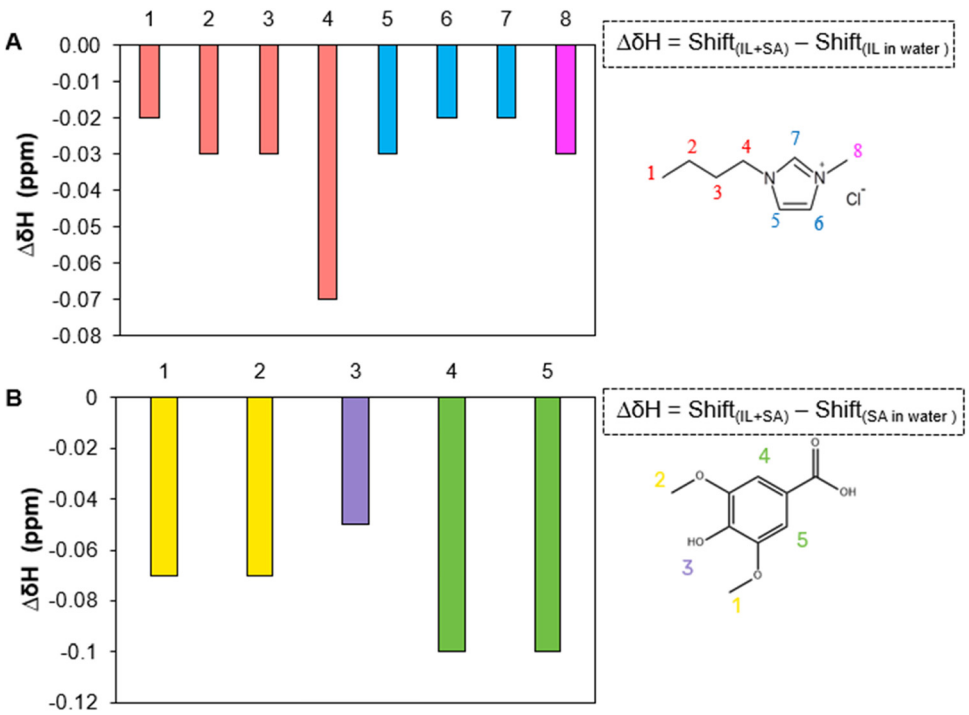

Fig. 5 (A) Proton chemical shifts ($\Delta\delta_H$) of the IL cation in a 1.0 mol L^{-1} solution of IL [C_4mim]Cl in water, saturated with syringic acid, compared to an aqueous solution of 1.0 mol L^{-1} IL solution without a solute. (B) Syringic acid molecule in saturated aqueous solution of 1.0 mol L^{-1} IL solution compared to syringic acid dissolved in water to saturation.

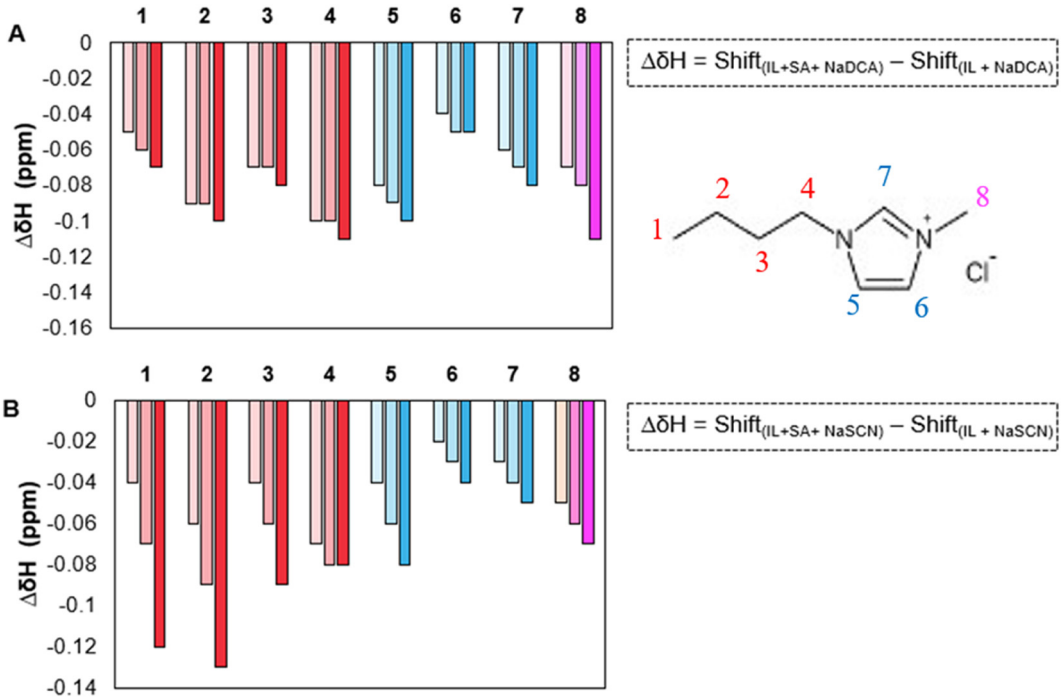

Fig. 6 (A) Proton chemical shifts ($\Delta\delta_H$) of the IL cation in a 1.0 mol L^{-1} solution of IL [C_4mim]Cl in 0.5 mol L^{-1} of Na[N(CN)$_2$] (light color), 1.0 mol L^{-1} of Na[N(CN)$_2$] (medium color) and 2.0 mol L^{-1} of Na[N(CN)$_2$] (dark color) in water, saturated with syringic acid, compared to an aqueous 1.0 mol L^{-1} IL solution with no solute. (B) Proton chemical shifts ($\Delta\delta_H$) of the IL cation in a 1.0 mol L^{-1} solution of IL [C_4mim]Cl in 0.5 mol L^{-1} of Na[SCN] (light color), 1.0 mol L^{-1} of Na[SCN] (medium color) and 2.0 mol L^{-1} of Na[SCN] (dark color) in water, saturated with syringic acid, compared to an aqueous 1.0 mol L^{-1} IL solution with no solute.

that hydrophobic interactions are the drivers of hydrotropy. Such behaviour is consistent with an increased pH contribution to syringic acid solubilisation, in which an increase in solubility is expected due to solute deprotonation, leading to the introduction of electrostatic and hydrogen-bonding interactions between the imidazolium cation and syringate anion in addition to dispersive ones. In contrast, a clear dependence on Na[SCN] concentration was observed for the terminal methyl and methylene groups of $[C_4mim]^+$ and is consistent with the increased self-aggregation of the IL in the presence of salt (formed NaCl) and solute addition.

The same solutions as shown in Fig. 6 were analyzed *via* DLS and the results concerning the hydrodynamic diameter of the aggregates in solution are presented in more detail in the ESI† (Fig. S4). For the (IL+ Na[N(CN)$_2$]) system in which the solubility is increased as the salt concentration is increased, the diameters of the aggregates at the different salt concentrations show a similar average distribution with maximum distribution shifts from 1.74 to 2.01 nm. For the (IL + Na[SCN]) system, the highest aggregate formation (approximately 3.61) is obtained in the IL + Na[SCN] 2.0 mol L^{-1} system, which is the system with the lowest solubilization of syringic acid, followed by IL + Na[SCN] 1.0 mol L^{-1} > IL + Na[SCN] 0.5 mol L^{-1}. To emphasize the solute aggregation process more clearly, Fig. 7 provides the correlation between aggregate formation in the Na[SCN] system and the $\Delta\delta_H$ chemical shifts of the imidazolium CH_3 group of the butyl chain. This illustration shows that the largest aggregates are formed when Na[SCN] is presented at a concentration of 2.0 mol L^{-1}. The tendency of syringic acid to segregate from solution in IL + salt is in agreement with the experimental observation that the solubility is lower in this system. From this aggregation promoted by Na[SCN], fewer IL cations remain available to participate in the hydrotropic solubilization of syringic acid, justifying the decreased solubilization in these systems.

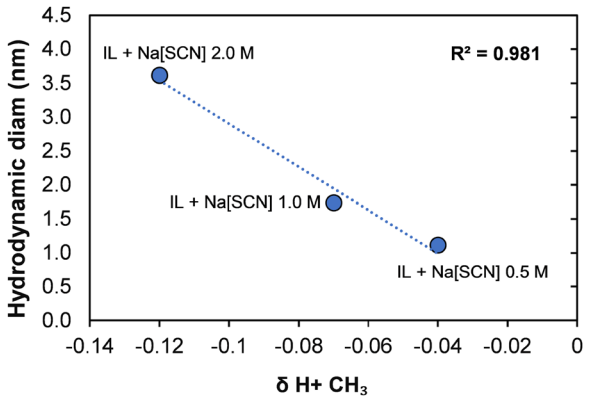

Fig. 7 Proton chemical shifts ($\Delta\delta_H$) of CH_3 IL in a 1.0 mol L^{-1} solution of IL [C_4mim]Cl in Na[SCN], saturated with syringic acid, relative to the diameters of the aggregates.

The ^{1}H-NMR and DLS analysis primarily focused on the solute–hydrotrope interactions *via* the IL cation. To fully understand the aggregation mechanism and the partition of the

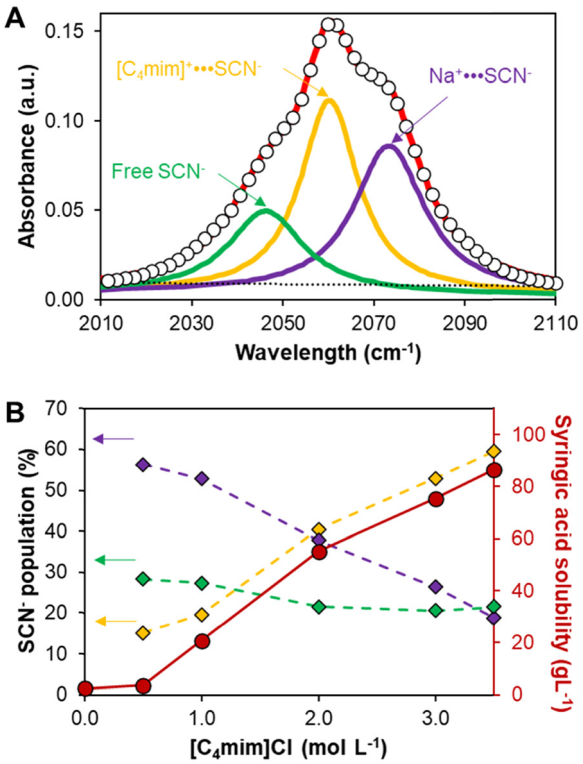

Fig. 8 (A) Example of deconvoluted Raman spectra at room temperature in the spectral range of the C≡N stretching mode of the cyanate-anions c for the system comprised of an equimolar ratio of $[C_4mim]Cl$ to Na[SCN] (Na[SCN] = 2.0 mol L^{-1}). The white circles correspond to the experimental spectra, whilst the red lines correspond to the cumulative spectra resulting from the individual band fits. (B) Evolution in $[SCN]^-$ speciation as a function of the $[C_4mim]Cl$ concentration (solute-free basis) for a fixed Na[SCN] concentration of 2.0 mol L^{-1} and the corresponding syringic acid solubility under these conditions. The colour code follows that of panel A. The normalised peak area for each composition is available in Table S7 (ESI†).

added salt anion, Raman spectroscopy was applied using the salt anion as the probe due to the sensitivity of the cyano band to its local environment. In this approach, the behaviour of the system $[C_4mim]Cl$ + Na[SCN] in aqueous solution at different IL and salt concentrations is investigated, focusing on the vibrational frequency of the totally symmetric mode, ω_{CN}, in the region 2040 to 2090 cm^{-1}. A characteristic spectrum in this region is presented in Fig. 8A along with an example of its deconvolution into three bands centered approximately around 2046 cm^{-1}, 2060 cm^{-1} and 2075 cm^{-1}. The band assignment is based on the work of Penna and co-workers,[55] in which the band for $[SCN]^-$ ions free of ionic pairing in solutions of organic solvents was observed at 2051 cm^{-1}.[56] Furthermore, the pure imidazolium thiocyanate IL exhibited a band at 2054 cm^{-1},[55] as indicated in their study and concentrated Na[SCN] melts displayed a band at 2074 cm^{-1} as per their findings.[57] The Raman spectrum was deconvoluted using the same criteria for all systems investigated, comprising $[C_4mim]Cl$ + Na[SCN] in aqueous solution at different IL concentrations with the results shown in Fig. 8B. In the quaternary systems composed of IL + Na[SCN] in water, a clear $[SCN]^-$ exchange is observed between Na^+ and $[C_4mim]^+$ as the concentration of the latter is increased. The results indicate increased ion-pairing between the IL cation and $[SCN]^-$ anion as more syringic acid is solubilised, stabilising the generated solute–hydrotrope aggregates. It does not appear that $[SCN]^-$ acts independently of $[C_4mim]^+$ cations to solubilise syringic acid. Instead, it appears that both ionic components contribute within a mixed aggregate, resulting in cation-rich and anion-rich aggregates.

Conclusions

The focus of this work was to investigate the behaviour of aqueous solutions of $[C_4mim]Cl$ with and without the presence of sodium salts and pH control on the solubility of syringic acid. The IL $[C_4mim]Cl$ in aqueous solution presents an excellent ability to increase the solubility of syringic acid up to 80 times. As a first approach in this work, the influence of the anion of sodium salts of the Hofmeister series was evaluated as an additive, and the solubility curve of $Na[N(CN)_2]$ and Na[SCN] at different concentrations was evaluated in more detail. A distinct mechanism of solubilization was found, in which the salting-in effect presented by the addition of $Na[N(CN)_2]$ corresponds mainly to the effect of pH. The addition of Na[SCN] to IL–hydrotropic solutions promotes a salting-out effect of syringic acid solubility when compared with the influence of the hydrotrope alone. The aggregation of ILs–ILs justifies the lower solubility observed upon the addition of Na[SCN] and highlights the impairment to hydrotropy when the aggregation of hydrotropes in solution occurs. The present results highlight the mechanism of hydrotropy proposed by Shimizu based on statistical thermodynamics, confirming hydrotropic solubilization resulting from solute aggregation driven by hydrophobic interactions.

Author contributions

Jordana Benfica: investigation, writing – original draft, data curation, software. Afonso C. Martins: investigation. German Sanchez-Perez: writing – review & editing. Seishi Shimizu: writing – review & editing. Nicolas Schaeffer: supervision, writing – review & editing. João A. P. Coutinho: supervision, project administration, writing – review & editing.

Conflicts of interest

There are no conflicts to declare.

Acknowledgements

This work was developed within the scope of the project CICECO-Aveiro Institute of Materials, UIDB/50011/2020, UIDP/50011/2020 & LA/P/0006/2020, financed by national funds through the Portuguese Foundation for Science and Technology/MCTES. J. B. S. acknowledges FCT for her PhD grant

2020.05802.BD. N. Schaeffer and G. Perez-Sanchez acknowledge the national funds (OE), through FCT (Fundação para a Ciência e a Tecnologia), in the scope of the framework contract foreseen in the numbers 4, 5 and 6 of the article 23, of the Decree-Law 57/2016, of August 29, changed by Law 57/2017, of July 19.

References

1 J. H. Clark, A. J. Hunt, C. Topi, G. Paggiola and J. Sherwood, in *Introduction to Solvents and Sustainable Chemistry*, ed. J. H. Clark, A. J. Hunt, C. Topi, G. Paggiola and J. Sherwood, 2017, pp. 1–34, DOI: 10.1039/9781782624035-00001.

2 E. Brini, C. J. Fennell, M. Fernandez-Serra, B. Hribar-Lee, M. Lukšič and K. A. Dill, How Water's Properties Are Encoded in Its Molecular Structure and Energies, *Chem. Rev.*, 2017, **117**(19), 12385–12414, DOI: 10.1021/acs.chemrev.7b00259.

3 M. Castro-Puyana, M. L. Marina and M. Plaza, Water as Green Extraction Solvent: Principles and Reasons for Its Use, *Curr. Opin. Green Sustainable Chem.*, 2017, **5**, 31–36, DOI: 10.1016/j.cogsc.2017.03.009.

4 A. D. Patel and M. A. Desai, Progress in the Field of Hydrotropy: Mechanism, Applications and Green Concepts, *Rev. Chem. Eng.*, 2022, **39**(4), 601–630, DOI: 10.1515/revce-2021-0012.

5 K. Häckl and W. Kunz, Some Aspects of Green Solvents, *C. R. Chim*, 2018, **21**(6), 572–580, DOI: 10.1016/j.crci.2018.03.010.

6 W. Kunz, K. Holmberg and T. Zemb, Hydrotropes, *Curr. Opin. Colloid Interface Sci.*, 2016, **22**, 99–107, DOI: 10.1016/j.cocis.2016.03.005.

7 M. Hopkins Hatzopoulos, J. Eastoe, P. J. Dowding, S. E. Rogers, R. Heenan and R. Dyer, Are Hydrotropes Distinct from Surfactants?, *Langmuir*, 2011, **27**(20), 12346–12353, DOI: 10.1021/la2025846.

8 T. F. Tadros, Aggregation of Surfactants, Self-Assembly Structures, Liquid Crystalline Phases, *An Introduction to Surfactants*, De Gruyter, 2014, pp. 29–50, DOI: 10.1515/9783110312133.29.

9 P. Bauduin, A. Renoncourt, A. Kopf, D. Touraud and W. Kunz, Unified Concept of Solubilization in Water by Hydrotropes and Cosolvents, *Langmuir*, 2005, **21**(15), 6769–6775, DOI: 10.1021/la050554l.

10 J. Y. Kim, S. Kim, M. Papp, K. Park and R. Pinal, Hydrotropic Solubilization of Poorly Water-Soluble Drugs, *J. Pharm. Sci.*, 2010, **99**(9), 3953–3965, DOI: 10.1002/jps.22241.

11 T. Buchecker, S. Krickl, R. Winkler, I. Grillo, P. Bauduin, D. Touraud, A. Pfitzner and W. Kunz, The Impact of the Structuring of Hydrotropes in Water on the Mesoscale Solubilisation of a Third Hydrophobic Component, *Phys. Chem. Chem. Phys.*, 2017, **19**(3), 1806–1816, DOI: 10.1039/C6CP06696H.

12 H. S. Frank and F. Franks, Structural Approach to the Solvent Power of Water for Hydrocarbons; Urea as a Structure Breaker, *J. Chem. Phys.*, 1968, **48**(10), 4746–4757, DOI: 10.1063/1.1668057.

13 J. G. Kirkwood and F. P. Buff, The Statistical Mechanical Theory of Solutions. I, *J. Chem. Phys.*, 1951, **19**(6), 774–777, DOI: 10.1063/1.1748352.

14 S. Shimizu and N. Matubayasi, The Origin of Cooperative Solubilisation by Hydrotropes, *Phys. Chem. Chem. Phys.*, 2016, **18**(36), 25621–25628, DOI: 10.1039/c6cp04823d.

15 D. O. Abranches, J. Benfica, B. P. Soares, A. Leal-Duaso, T. E. Sintra, E. Pires, S. P. Pinho, S. Shimizu and J. A. P. Coutinho, Unveiling the Mechanism of Hydrotropy: Evidence for Water-Mediated Aggregation of Hydrotropes around the Solute, *Chem. Commun.*, 2020, **56**(52), 7143–7146, DOI: 10.1039/d0cc03217d.

16 P. Bauduin, A. Renoncourt, A. Kopf, D. Touraud and W. Kunz, Unified Concept of Solubilization in Water by Hydrotropes and Cosolvents, *Langmuir*, 2005, **21**(15), 6769–6775, DOI: 10.1021/LA050554L.

17 A. M. Hyde, S. L. Zultanski, J. H. Waldman, Y.-L. Zhong, M. Shevlin and F. Peng, General Principles and Strategies for Salting-Out Informed by the Hofmeister Series, *Org. Process Res. Dev.*, 2017, **21**(9), 1355–1370, DOI: 10.1021/acs.oprd.7b00197.

18 A. Kalra, N. Tugcu, S. M. Cramer and S. Garde, Salting-in and Salting-out of Hydrophobic Solutes in Aqueous Salt Solutions, *J. Phys. Chem. B*, 2001, **105**(27), 6380–6386, DOI: 10.1021/jp010568.

19 S. Endo, A. Pfennigsdorff and K. U. Goss, Salting-out Effect in Aqueous NaCl Solutions: Trends with Size and Polarity of Solute Molecules, *Environ. Sci. Technol.*, 2012, **46**(3), 1496–1503, DOI: 10.1021/es203183z.

20 J. Mehringer and W. Kunz, Carl Neuberg's Hydrotropic Appearances (1916), *Adv. Colloid Interface Sci.*, 2021, **294**, 102476, DOI: 10.1016/J.CIS.2021.102476.

21 G. Grundl, M. Müller, D. Touraud and W. Kunz, Salting-out and Salting-in Effects of Organic Compounds and Applications of the Salting-out Effect of Pentasodium Phytate in Different Extraction Processes, *J. Mol. Liq.*, 2017, **236**, 368–375, DOI: 10.1016/J.MOLLIQ.2017.03.091.

22 L. M. Pegram and M. T. Record, Hofmeister Salt Effects on Surface Tension Arise from Partitioning of Anions and Cations between Bulk Water and the Air-Water Interface, *J. Phys. Chem. B*, 2007, **111**(19), 5411–5417, DOI: 10.1021/JP070245Z.

23 A. F. M. Cláudio, M. C. Neves, K. Shimizu, J. N. Canongia Lopes, M. G. Freire and J. A. P. Coutinho, The Magic of Aqueous Solutions of Ionic Liquids: Ionic Liquids as a Powerful Class of Catanionic Hydrotropes, *Green Chem.*, 2015, **17**(7), 3948–3963, DOI: 10.1039/C5GC00712G.

24 K. I. Assaf and W. M. Nau, The Chaotropic Effect as an Assembly Motif in Chemistry, *Angew. Chem., Int. Ed.*, 2018, **57**(43), 13968–13981, DOI: 10.1002/anie.201804597.

25 C. Drummond, L. Pérez-Fuentes and D. Bastos-González, Can Polyoxometalates Be Considered as Superchaotropic Ions?, *J. Phys. Chem. C*, 2019, **123**(47), 28744–28752, DOI: 10.1021/acs.jpcc.9b08324.

26 I. Chazapi, O. Diat and P. Bauduin, Aqueous Solubilization of Hydrophobic Compounds by Inorganic Nano-Ions: An

Unconventional Mechanism, *J. Colloid Interface Sci.*, 2023, **638**, 561–568, DOI: 10.1016/j.jcis.2023.01.115.

27 T. E. Sintra, K. Shimizu, S. P. M. Ventura, S. Shimizu, J. N. Canongia Lopes and J. A. P. Coutinho, Enhanced Dissolution of Ibuprofen Using Ionic Liquids as Catanionic Hydrotropes, *Phys. Chem. Chem. Phys.*, 2018, **20**(3), 2094–2103, DOI: 10.1039/C7CP07569C.

28 I. Sales, D. O. Abranches, P. Costa, T. E. Sintra, S. P. M. Ventura, S. Mattedi, J. A. P. Coutinho, M. G. Freire and S. P. Pinho, Enhancing Artemisinin Solubility in Aqueous Solutions: Searching for Hydrotropes Based on Ionic Liquids, *Fluid Phase Equilib.*, 2021, **534**, 112961, DOI: 10.1016/j.fluid.2021.112961.

29 D. O. Abranches, J. Benfica, B. P. Soares, A. M. Ferreira, T. E. Sintra, S. Shimizu and J. A. P. Coutinho, The Impact of the Counterion in the Performance of Ionic Hydrotropes, *Chem. Commun.*, 2021, **57**(23), 2951–2954, DOI: 10.1039/D0CC08092F.

30 D. R. MacFarlane, M. Forsyth, E. I. Izgorodina, A. P. Abbott, G. Annat and K. Fraser, On the Concept of Ionicity in Ionic Liquids, *Phys. Chem. Chem. Phys.*, 2009, **11**(25), 4962, DOI: 10.1039/b900201d.

31 D. Lengvinaitė, S. Kvedaraviciute, S. Bielskutė, V. Klimavicius, V. Balevicius, F. Mocci, A. Laaksonen and K. Aidas, Structural Features of the [C4mim][Cl] Ionic Liquid and Its Mixtures with Water: Insight from a ^{1}H NMR Experimental and QM/MD Study, *J. Phys. Chem. B*, 2021, **125**(48), 13255–13266, DOI: 10.1021/acs.jpcb.1c08215.

32 B. Kang, H. Tang, Z. Zhao and S. Song, Hofmeister Series: Insights of Ion Specificity from Amphiphilic Assembly and Interface Property, *ACS Omega*, 2020, **5**(12), 6229–6239, DOI: 10.1021/acsomega.0c00237.

33 A. C. Martins, J. Benfica, G. Perez-Sanchez, S. Shimizu, T. Sintra, N. Schaeffer and J. A. P. Coutinho, Assessing the Hydrotropic Effect in the Presence of Electrolytes: Competition between Solute Salting-out and Salt-Induced Hydrotrope Aggregation, *Phys. Chem. Chem. Phys.*, 2022, **24**, 21645–21654, DOI: 10.1039/D2CP00749E.

34 B. P. Soares, D. O. Abranches, T. E. Sintra, A. Leal-Duaso, J. I. García, E. Pires, S. Shimizu, S. P. Pinho and J. A. P. Coutinho, Glycerol Ethers as Hydrotropes and Their Use to Enhance the Solubility of Phenolic Acids in Water, *ACS Sustainable Chem. Eng.*, 2020, **8**(14), 5742–5749, DOI: 10.1021/acssuschemeng.0c01032.

35 R. Sadeghi and F. Jahani, Salting-in and Salting-out of Water-Soluble Polymers in Aqueous Salt Solutions, *J. Phys. Chem. B*, 2012, **116**(17), 5234–5241, DOI: 10.1021/jp300665b.

36 J. Setschenow, Über Die Konstitution Der Salzlösungen Auf Grund Ihres Verhaltens Zu Kohlensäure, *Zeitschrift für Physikalische Chemie*, 1889, **4U**(1), 117–125, DOI: 10.1515/zpch-1889-0409.

37 P. M. Gross, The ''Salting out'' of Non-Electrolytes from Aqueous Solutions, *Chem. Rev.*, 1933, **13**(1), 91–101, DOI: 10.1021/CR60044A007.

38 H. D. B. Jenkins, H. K. Roobottom, J. Passmore and L. Glasser, Relationships among Ionic Lattice Energies, Molecular (Formula Unit) Volumes, and Thermochemical Radii, *Inorg. Chem.*, 1999, **38**(16), 3609–3620, DOI: 10.1021/ic9812961.

39 J. M. Slattery, C. Daguenet, P. J. Dyson, T. J. S. Schubert and I. Krossing, How to Predict the Physical Properties of Ionic Liquids: A Volume-Based Approach, *Angew. Chem., Int. Ed.*, 2007, **46**(28), 5384–5388, DOI: 10.1002/anie.200700941.

40 Y. Marcus, Thermodynamics of Solvation of Ions. Part 5.—Gibbs Free Energy of Hydration at 298.15 K, *J. Chem. Soc., Faraday Trans.*, 1991, **87**(18), 2995–2999, DOI: 10.1039/FT9918702995.

41 P. Naert, K. Rabaey and C. V. Stevens, Ionic Liquid Ion Exchange: Exclusion from Strong Interactions Condemns Cations to the Most Weakly Interacting Anions and Dictates Reaction Equilibrium, *Green Chem.*, 2018, **20**(18), 4277–4286, DOI: 10.1039/C8GC01869C.

42 E. Furia, A. Beneduci, L. Malacaria, A. Fazio, C. la Torre and P. Plastina, Modeling the Solubility of Phenolic Acids in Aqueous Media at 37 °C, *Molecules*, 2021, **26**(21), 6500, DOI: 10.3390/molecules26216500.

43 F. Erdemgil, S. Sanli, N. Sanli, G. Ozkan, J. Barbosa, J. Guiteras and J. Beltran, Determination of PKa Values of Some Hydroxylated Benzoic Acids in Methanol–Water Binary Mixtures by LC Methodology and Potentiometry, *Talanta*, 2007, **72**(2), 489–496, DOI: 10.1016/j.talanta.2006.11.007.

44 M. Abdul Rub and D. Kumar, Micellization Behavior of Antidepressant Imipramine Hydrochloride Drug and Hydrotrope (Sodium Tosylate) Mixtures at Different Compositions and Temperatures in Different Media, *J. Chem. Eng. Data*, 2020, **65**(5), 2659–2672, DOI: 10.1021/ACS.JCED.0C00038.

45 T. E. Sintra, A. Luís, S. N. Rocha, A. I. M. C. Lobo Ferreira, F. Gonçalves, L. M. N. B. F. Santos, B. M. Neves, M. G. Freire, S. P. M. Ventura and J. A. P. Coutinho, Enhancing the Antioxidant Characteristics of Phenolic Acids by Their Conversion into Cholinium Salts, *ACS Sustainable Chem. Eng.*, 2015, **3**(10), 2558–2565, DOI: 10.1021/acssuschemeng.5b00751.

46 Y. Cao and T. Mu, Comprehensive Investigation on the Thermal Stability of 66 Ionic Liquids by Thermogravimetric Analysis, *Ind. Eng. Chem. Res.*, 2014, **53**(20), 8651–8664, DOI: 10.1021/ie5009597.

47 A. F. M. Cláudio, M. C. Neves, K. Shimizu, J. N. Canongia Lopes, M. G. Freire and J. A. P. Coutinho, The Magic of Aqueous Solutions of Ionic Liquids: Ionic Liquids as a Powerful Class of Catanionic Hydrotropes, *Green Chem.*, 2015, **17**(7), 3948–3963, DOI: 10.1039/c5gc00712g.

48 R. Hayes, G. G. Warr and R. Atkin, Structure and Nanostructure in Ionic Liquids, *Chem. Rev.*, 2015, **115**(13), 6357–6426, DOI: 10.1021/cr500411q.

49 M. Blesic, M. H. Marques, N. V. Plechkova, K. R. Seddon, L. P. N. Rebelo and A. Lopes, Self-Aggregation of Ionic Liquids: Micelle Formation in Aqueous Solution, *Green Chem.*, 2007, **9**(5), 481, DOI: 10.1039/b615406a.

50 C. Jungnickel, J. Łuczak, J. Ranke, J. F. Fernández, A. Müller and J. Thöming, Micelle Formation of Imidazolium Ionic Liquids in Aqueous Solution, *Colloids Surf., A*, 2008, **316**(1–3), 278–284, DOI: 10.1016/j.colsurfa.2007.09.020.

51 I. Goodchild, L. Collier, S. L. Millar, I. Prokeš, J. C. D. Lord, C. P. Butts, J. Bowers, J. R. P. Webster and R. K. Heenan, Structural Studies of the Phase, Aggregation and Surface Behaviour of 1-Alkyl-3-Methylimidazolium Halide + Water Mixtures, *J. Colloid Interface Sci.*, 2007, **307**(2), 455–468, DOI: **10.1016/j.jcis.2006.11.034**.

52 E. A. Crespo, N. Schaeffer, J. A. P. Coutinho and G. Perez-Sanchez, Improved Coarse-Grain Model to Unravel the Phase Behavior of 1-Alkyl-3-Methylimidazolium-Based Ionic Liquids through Molecular Dynamics Simulations, *J. Colloid Interface Sci.*, 2020, **574**, 324–336, DOI: **10.1016/j.jcis.2020.04.063**.

53 H. Wang, Q. Feng, J. Wang and H. Zhang, Salt Effect on the Aggregation Behavior of 1-Decyl-3-Methylimidazolium Bromide in Aqueous Solutions, *J. Phys. Chem. B*, 2010, **114**(3), 1380–1387, DOI: **10.1021/jp910903s**.

54 D. O. Abranches, J. Benfica, S. Shimizu and J. A. P. Coutinho, The Perspective of Cooperative Hydrotropy on the Solubility in Aqueous Solutions of Cyrene, *Ind. Eng. Chem. Res.*, 2020, **59**(41), 18649–18658, DOI: **10.1021/ACS.IECR.0C02346**.

55 T. C. Penna, L. F. O. Faria and M. C. C. Ribeiro, Raman Band Shape Analysis of Cyanate-Anion Ionic Liquids, *J. Mol. Liq.*, 2015, **209**, 676–682, DOI: **10.1016/j.molliq.2015.06.038**.

56 M. Chabanel, A. Bencheikh and D. Puchalska, Vibrational Study of Ionic Association in Aprotic Solvents. Part 12. Isothiocyanate M(NCS) Complexes of Non-Transition-Metal Ions, *J. Chem. Soc., Dalton Trans.*, 1989, **11**, 2193, DOI: **10.1039/dt9890002193**.

57 C. B. Baddiel and G. J. Janz, Molten Thiocyanates: Raman Spectra and Structure, *Trans. Faraday Soc.*, 1964, **60**, 2009, DOI: **10.1039/tf9646002009**.

